Ascorbate oxidase: The unexpected involvement of a ‘wasteful enzyme’ in the symbioses with nitrogen-fixing bacteria and arbuscular mycorrhizal fungi

- Raffaella Balestrini[a, e],
- Thomas Ott[b],
- Mike Güther[a, e, 1],
- Paola Bonfante[a, e],
- Michael K. Udvardi[c],
- Mario C. De Tullio[d, ,

Abstract

Ascorbate oxidase (AO, EC 1.10.3.3) catalyzes the oxidation of ascorbate (AsA) to yield water. AO over-expressing plants are prone to ozone and salt stresses, whereas lower expression apparently confers resistance to unfavorable environmental conditions. Previous studies have suggested a role for AO as a regulator of oxygen content in photosynthetic tissues. For the first time we show here that the expression of a *Lotus japonicus* AO gene is induced in the symbiotic interaction with both nitrogen-fixing bacteria and arbuscular mycorrhizal (AM) fungi. In this framework, high AO expression is viewed as a possible strategy to down-regulate oxygen diffusion in root nodules, and a component of AM symbiosis. A general model of AO function in plants is discussed.

Highlights

► AO catalyzes the oxidation of ascorbate and the reduction of O_2 to water. ► The expression of a *Lotus japonicus* AO is induced in the symbiosis with rhizobia and AM fungi. ► AO could be involved in the control of oxygen diffusion and in redox signaling modules.

Keywords

- Ascorbate;
- Ascorbate oxidase;
- Oxygen;
- Plant–microorganism interaction;
- Root nodules;
- Arbuscular mycorrhizal fungi;
- Signaling

1. Introduction

More than 80 years after its discovery as ‘hexoxidase’ [1], the function of ascorbate oxidase (AO, EC 1.10.3.3) is still controversial [2]. In most cases, the physiological role of an enzyme is written in the reaction it catalyzes, namely in the reagents used and the products yielded. Therefore, the function of an enzyme catalyzing the waste (oxidation) of ascorbate (AsA) to reduce oxygen to water is quite hard to explain. AO over-expressing plants are prone to ozone [3] and salt [4] stresses, whereas lower expression apparently confers resistance to unfavorable environmental conditions [4]. Therefore, AO activity appears at best not necessary, if not even dangerous, and the silencing of AO genes seems a valuable strategy to increase AsA content in crops [5]. In this context, the widespread presence of multiple copies of putative AO-encoding genes in virtually all plant taxa, as evidenced by EST analysis, seems inexplicable. No surprise that AO has been defined a ‘mysterious enzyme’ [6].

Several hypotheses have been advanced to explain AO function [2]. Between the 1960s and the beginning of the new century, the opinion prevailed that AO controls cell extension, although the actual mechanism of its action remained unknown [7], [8] and [9]. Gene expression analysis showed that the AO gene is induced by light [10] and [11]. Further studies on the effects of AO overexpression in tobacco [12] revealed that the enzyme affects the apoplast redox state, activating a signal transduction mechanism affecting the expression of relevant genes involved in plant growth and defense responses.

A different line of research explored the involvement of AO in controlling oxygen concentration under specific conditions [2] and [11]. Data on light-induced expression of AO support the hypothesis of a mechanism acting to remove excess oxygen produced in the photosynthetic process. AO activity also increased when plants were exposed to higher O_2 levels in the dark [11]. However, the ‘oxygen connection’ hypothesis requires additional experimental support.

Plants have to cope with oxygen in many ways. A tight control over oxygen diffusion and the formation of reactive oxygen species (ROS) is also necessary in plant–microbe interaction, since the nitrogen-fixing enzyme nitrogenase is dramatically inactivated by even low oxygen concentrations. For this purpose, both anatomical and functional means for O_2 containment occur in nodules. An oxygen diffusion barrier (ODB) [13], [14] and [15] is localized to the peripheral cell layers around the endodermis of the nodule [16] and is involved in restricting oxygen entry. In spite of extensive studies, detailed functional characterization of ODB is still lacking. Even less is known about the possible role of oxygen in the establishment of the interaction with arbuscular mycorrhizal (AM) fungi, although it is widely known that the AM symbiosis share some molecular responses with nodule formation.

Here we report the identification and partial characterization of a symbiosis-induced AO gene overexpressed in *Lotus japonicus* during its interaction with either N_2-fixing *Mesorhizobium loti* or the AM fungus *Gigaspora margarita*. Both the AO gene expression pattern and the localization of the AO protein in nodule ODB and in the AM perifungal space support the hypothesis of a key role of this gene/enzyme in both nodule and AM development and functioning.

2. Results

2.1. Identification of LjAO1, a gene encoding an ascorbate oxidase

A cDNA array experiment using 9652 nodule-derived EST clones spotted on a nylon membrane identified several genes induced upon rhizobial inoculation [17], [18] and [19]. Among them, the clone LjNEST98c11r (Genbank accession CB829448) was identified, which was transcriptionally induced during nodule development. Searching the current genome annotation of *Lotus japonicus* (version 2.5; http://www.kazusa.or.jp/lotus/) yielded the full-length sequence of gene chr2.CM0504.260.r2.m encoding a putative ascorbate oxidase (*LjAO1*). However, the current annotation contains several stop codons in the 5′ region of the putative coding sequence (CDS). To reveal the true length of the transcript we identified the closest homologous sequences in *Medicago truncatula* (AC235679_6.1; www.medicago.org) [20] and *Glycine max* (Glyma14g04530.1 (581 amino acids) and Glyma20g12220.1 (574 amino acids) by using the translated sequence of EST LjNEST98c11r as a template. To unravel the sequence of the 5′ region of *LjAO1* we performed 5′ RACE PCR on cDNA obtained from mature, 21 days old nodules of wild-type *L. japonicus*. Finally, sequence analysis and assembly of a consensus contig of the obtained fragments resulted in a putative full-length CDS of 1707 bp encoding a 568 amino acid long LjAO1 protein (GenBank accession number: JX312221) sharing 80.1% similarity (66.8% identity) to *M. truncatula* AC235679_6.1 and 81.8% similarity (69.3% identity) to the soybean Glyma20g12220.1 protein.

The putative full-length pre-mature mRNA sequence including its full 3′ UTR was used for signal peptide predictions using TargetP V1.0 (http://www.cbs.dtu.dk/services/TargetP/) and PSORT (http://psort.nibb.ac.jp/) softwares. Both softwares predicted signal peptides characteristic for secretory pathways and extracellular localization with a probability of 0.983 and 0.814, respectively.

2.2. LjAO1 expression is induced during nodulation and localizes around the nodule endodermis

LjAO1 expression was monitored in different plant organs and during nodule development by qRT-PCR. Plants were grown *in vitro* for 2 weeks prior to inoculation with rhizobia. Control plants were inoculated with a mock solution. Uninoculated and inoculated roots were harvested 7, 14 and 21 days post inoculation (Fig. 1A). As the induction of *LjAO1* expression could already be detected as early as 1 dpi, this gene can be classified as an early nodulin.

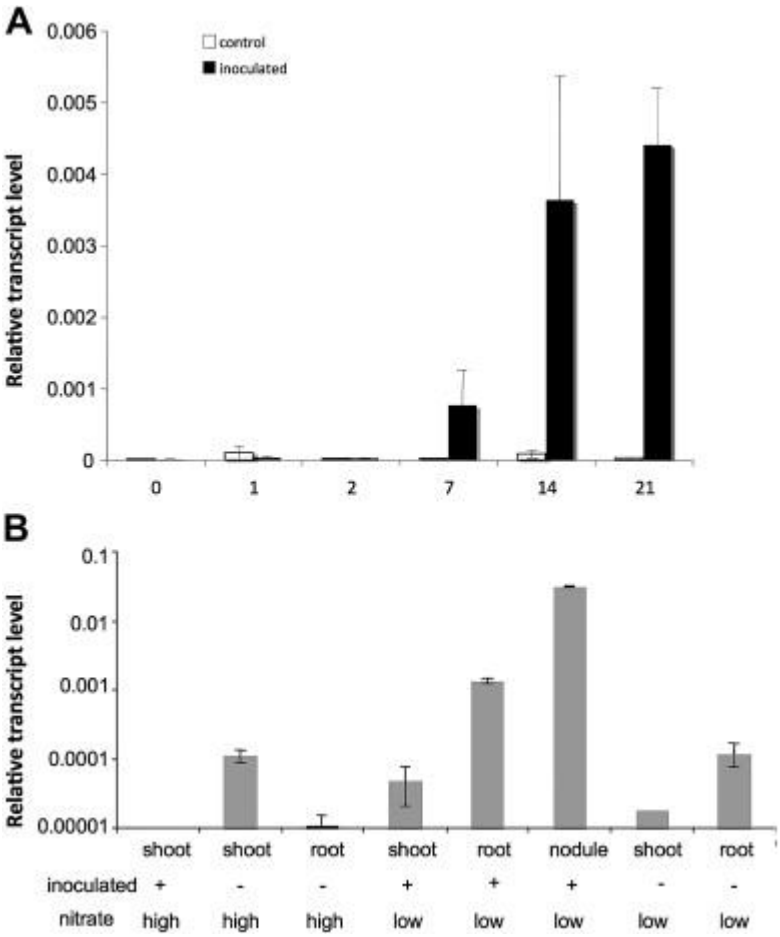

Fig. 1.

Relative transcript level of *LjAO1* during nodule development. A. Relative transcript level of *LjAO1* was determined for inoculated roots plus nodules and uninoculated roots (controls) of *Lotus japonicus* using qRT-PCR. Tissue was harvested at the time points indicated between 0 and 21 days post inoculation. 8–10 plants were pooled per replicate prior to RNA extraction. Expression levels of *LjAO1* were normalized in relation to a housekeeping gene (ubiquitin). Error bars represent the standard deviation of six measurements. B. Expression of *LjAO1* in different plant organs. Plants were grown on 5.0 mM (high) and 0.1 mM (low) KNO_3 for three weeks under symbiotic (+) and nonsymbiotic conditions (−). Shoots and leaves, roots and nodules were harvested separately. Material was harvested and pooled from 8 to 10 individual plants. Error bars indicate standard deviation. Expression levels of *LjAO1* were normalized and expressed relative to ubiquitin.

Different plant organs were harvested 21 dpi and RNA was extracted from all tissues (Fig. 1B). Transcript levels were 11-fold higher in roots of uninoculated plants grown for 21 days on 0.1 mM KNO3 (low nitrate) compared to plants of the same age grown on 5.0 mM KNO3 (high nitrate). Transcript abundance of *LjAO1* was more than 200-fold higher in nodules than in any other organ. Expression levels in infected roots and nodules were higher than in shoot and leaf material harvested from the same plants. *LjAO1* transcript levels in roots increased following inoculation with rhizobia to values 850-fold higher than in uninoculated controls 21 dpi (Fig. 1B). Interestingly, when plants were inoculated with the *cgs* mutant strain of *M. loti*, which is affected in the synthesis of cyclic β(1–2) glucan and unable to form nodules [18], AO expression was 7-fold lower than in plants inoculated with the WT strain (data not shown).

In order to refine the data obtained from expression analysis and to study the spatial expression of LjAO1 within nodule and root tissue, we used genomic information to select a putative promoter region of about 1600 bp. Part of the promoter region (1049 bp upstream of the predicted start codon) was amplified by PCR, fused to the GUS gene in the cloning vector pBI101 and transformed into *Agrobacterium rhizogenes* for hairy root transformation. GUS staining of transformed roots revealed reporter gene expression almost exclusively in the nodules and rarely in root tips and the vascular tissue of lateral roots (Fig. 2). GUS activity was localiszed to a ring of cells in the periphery of the nodules (Fig. 2A). This pattern was also evident in sections of embedded material, which revealed more clearly expression in the endodermal and subendodermal cell layers (Fig. 2B, C). Infected and uninfected cells of the inner cortex did not show GUS-staining.

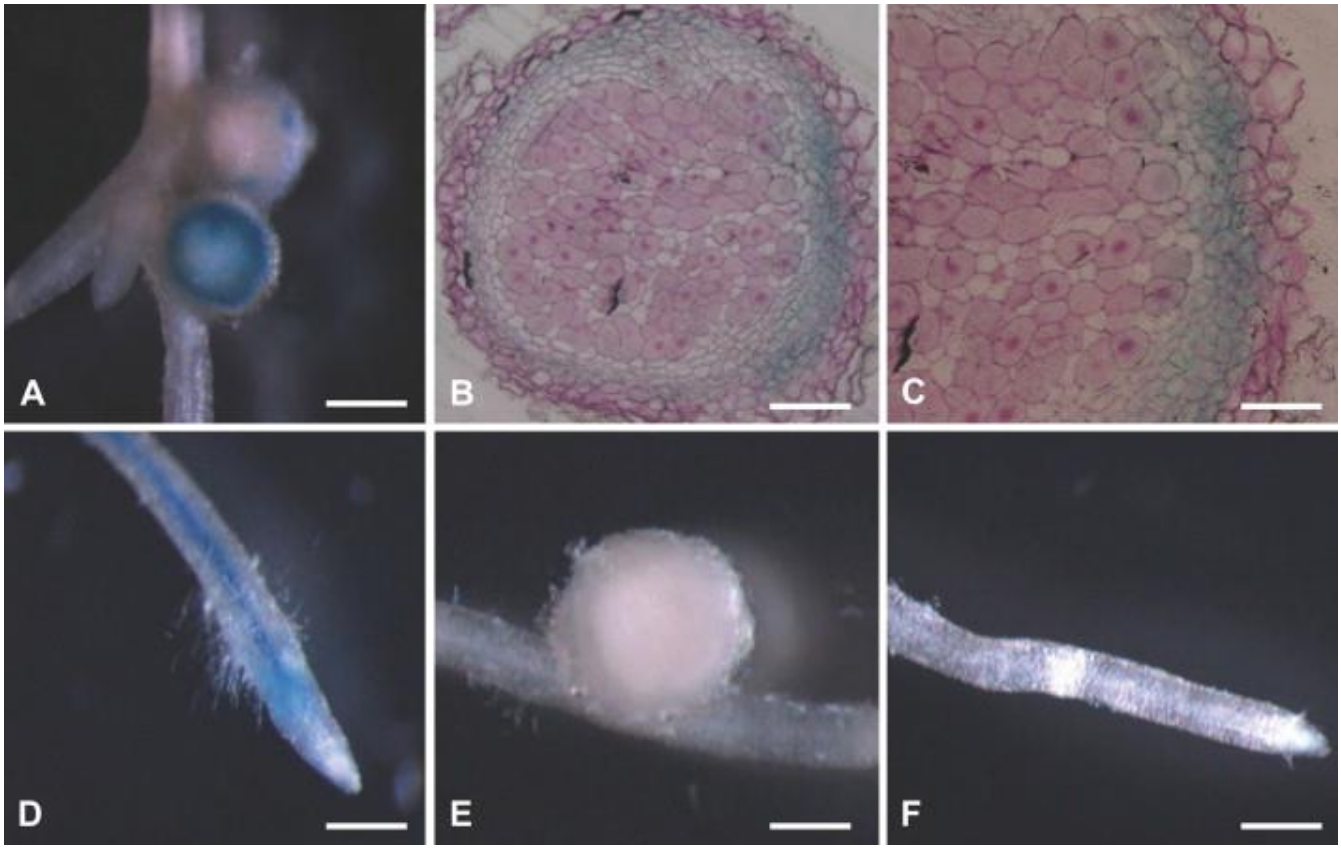

Fig. 2.

Promoter analysis of *LjAO1* using hairy root transformation. *Lotus japonicus* was transformed with *Agrobacterium rhizogenes* carrying a 1049 bp long fragment of the *LjAO1* promoter fused to the *Gus* gene. Gus staining was detected in the periphery of transgenic nodules (A, B, C) and rarely in secondary roots (D). B and C. Embedded cross-sections of nodules show Gus-staining in cell layers of the nodule endodermis. E and F. Controls were transformed with the pBI101 vector alone. Bars = 1400, 350 and 150 μm in A, B and C respectively; 700 μm in D, E, F.

Putative regulatory elements in the cloned promoter region were identified using the PLACE software (http://www.dna.affrc.go.jp/PLACE/signalscan.html). Several potential regulatory motifs were found, including motifs such as “AAAGAT” and “CTCTT” previously described as nodulin consensus sequences [21] and [22].

2.3. LjAO1 expression is induced in mycorrhizal roots

Quantitative RT-PCR experiments were carried out to verify mRNA expression levels of *LjAO1*. The absence of cross-hybridization with fungal template was demonstrated by PCR on genomic DNA of *Gigaspora margarita*. The negative results obtained from such control amplifications allowed us to exclude any cross hybridization with the fungal genome. cDNAs were obtained from mycorrhizal and non mycorrhizal roots and used as templates to follow the *LjAO1* expression. As shown in Fig. 3A, *LjAO1* transcripts were more than 12-fold higher in mycorrhizal roots than in non-mycorrhizal ones.

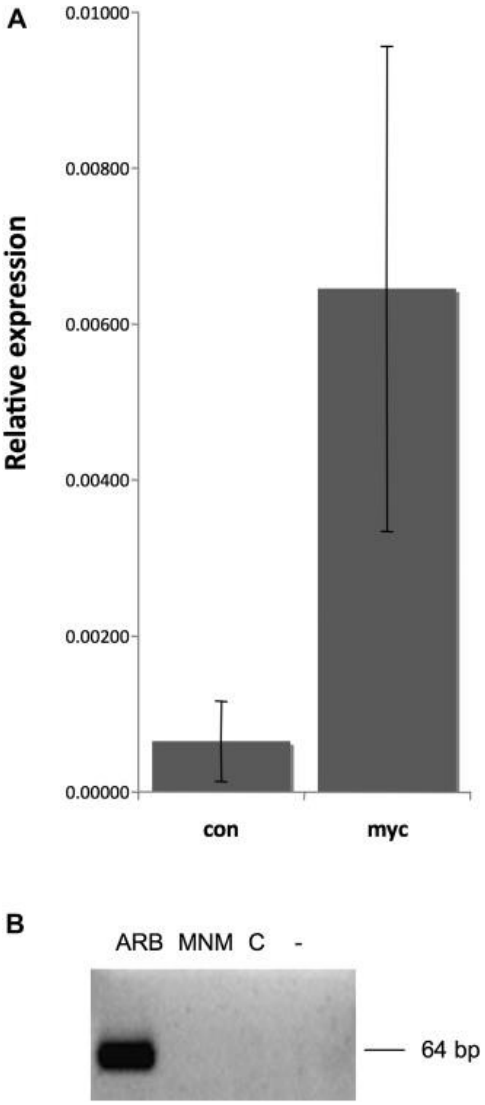

Fig. 3.

Transcript accumulation of ascorbate oxidase gene upon inoculation with *Gi. margarita*. A. *LjAO1* gene expression was analyzed by qRT-PCR in non-mycorrhizal (con) and mycorrhizal roots (myc). Data were calibrated by the expression values obtained for an ubiquitin gene (*LjUBQ10*, TC14054). Mean values are shown with SEs from three independent root inoculations. B. RT-PCR analysis of microdissected cells with *LjAO1* primers. An amplified fragment of the expected size is present exclusively in arbusculated cell population. C, cortical cells from non-mycorrhizal roots; MNM, non-colonized cortical cells from mycorrhizal roots; ARB, arbusculated cortical cells; −, negative control.

2.4. Detection of LjAO1 transcripts in microdissected samples

One-step RT-PCR assays were carried out in order to detect *LjAO1* transcripts in RNAs from the several microdissected cell-type populations: cortical cells from non-mycorrhizal roots (C); non-colonized cortical cells from mycorrhizal roots (MNM) and arbuscule-containing cells (ARB). RT-PCR reactions on microdissected samples highlighted the presence of *LjAO1* transcripts exclusively in arbuscule-containing cells (Fig. 3B). The absence of an amplified product in RT *minus* reactions excluded any DNA contamination. By contrast, an amplified fragment of the expected size was observed in all the cell populations using specific primers for *EF* (data not shown).

2.5. Protein localization in nodules and mycorrhizal roots

In semithin sections, *L. japonicus* nodules typically show a large, central, infected zone surrounded by the uninfected nodule cortex (Fig. 4A). In the infected cells, several bacteroids are present in a symbiosome (Fig. 4B). The anti-AO antibody was used in immunogold experiments in order to detect the distribution of the proteins in the *L. japonicus* nodules. Electron microscopy shows that anti-AO led to an intense labeling in the intercellular spaces of the peripheral tissues (Fig. 4C). Gold granules were found also in vacuoles and on membranous structures. In infected tissue, gold granules were present in the peribacteroid space and an abundant labeling is associated with electrondense material (Fig. 4D, E). The labeling was particularly abundant when the symbiosomes were cut in a region without bacteria (Fig. 4E, F). No labeling was present in a control section where the primary antibody was omitted (Fig. 4G).

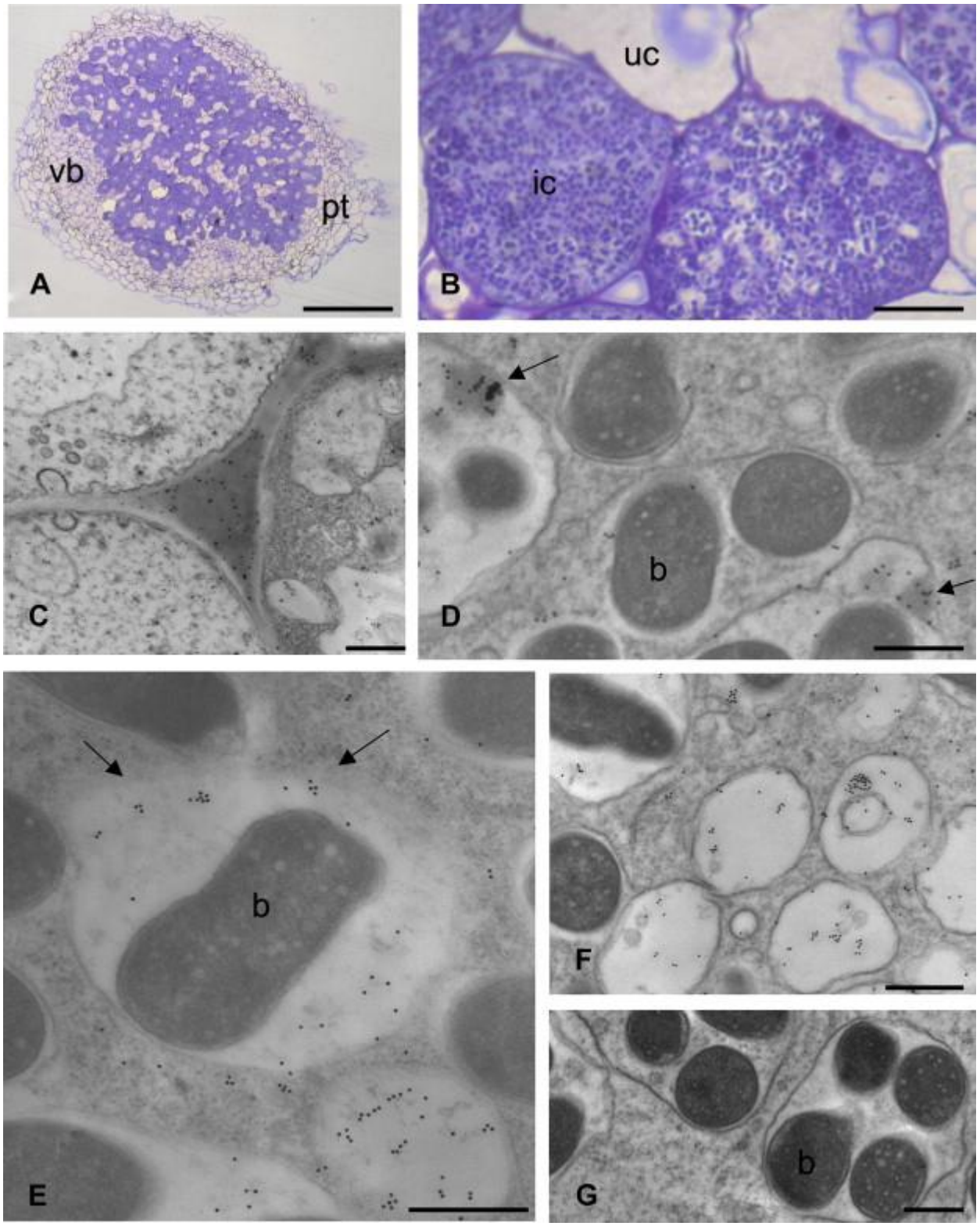

Fig. 4.

Detection of ascorbate oxidase in *L. japonicus* nodules. A. Semithin section of a determinate globose nodule of *Lotus japonicus* containing a large, central, infected zone surrounded by the uninfected nodule cortex. vb, vascular bundle; pt, peripheral tissue. Bar = 100 μm. B. Magnification of the infected zone. UC, uninfected cells; IC, infected cells. Bar = 10 μm. C–F. Immunogold localization of ascorbate oxidase. In the peripheral tissue an abundant labeling is present on the intercellular spaces (asterisk). Gold particles were also evident in vacuoles and on membranous structures. D–E. In infected tissue, more bacteroids are

present in a symbiosome. Gold granules are present in the peribacteroid space (arrows) and an abundant labeling is associated with electrondense material (C, arrowheads). F. Gold granules are particularly abundant when the symbiosomes were cut in a region without bacteria. G. No labeling was present in a control section where the primary antibody was omitted. Bars = 0.5 μm.

The mycorrhizal phenotype in *L. japonicus* has been described in detail elsewhere [23] and [24]. The most important features of the colonization process are visible on semithin sections. The fungus proceeds through epidermal cells to the outer cortex, via intracellular hyphae; then they become intercellular at the contact with the inner cortical layer, where they re-enter and eventually produce abundant arbuscules (Fig. 5A, B). Upon colonization by the AM fungus, the anti-AO led to a labeling in the interface region space around the hyphae (Fig. 5C, E), which is the space surrounded by the perifungal membrane of host origin and the fungal wall. Labeling was present around both the active fungal hyphae (Fig. 5D) and the collapsed ones (Fig. 5E). Gold granules were also found in the intercellular spaces between cortical cells and in vacuoles (data not shown), in accordance with previous observations on cucumber [25].

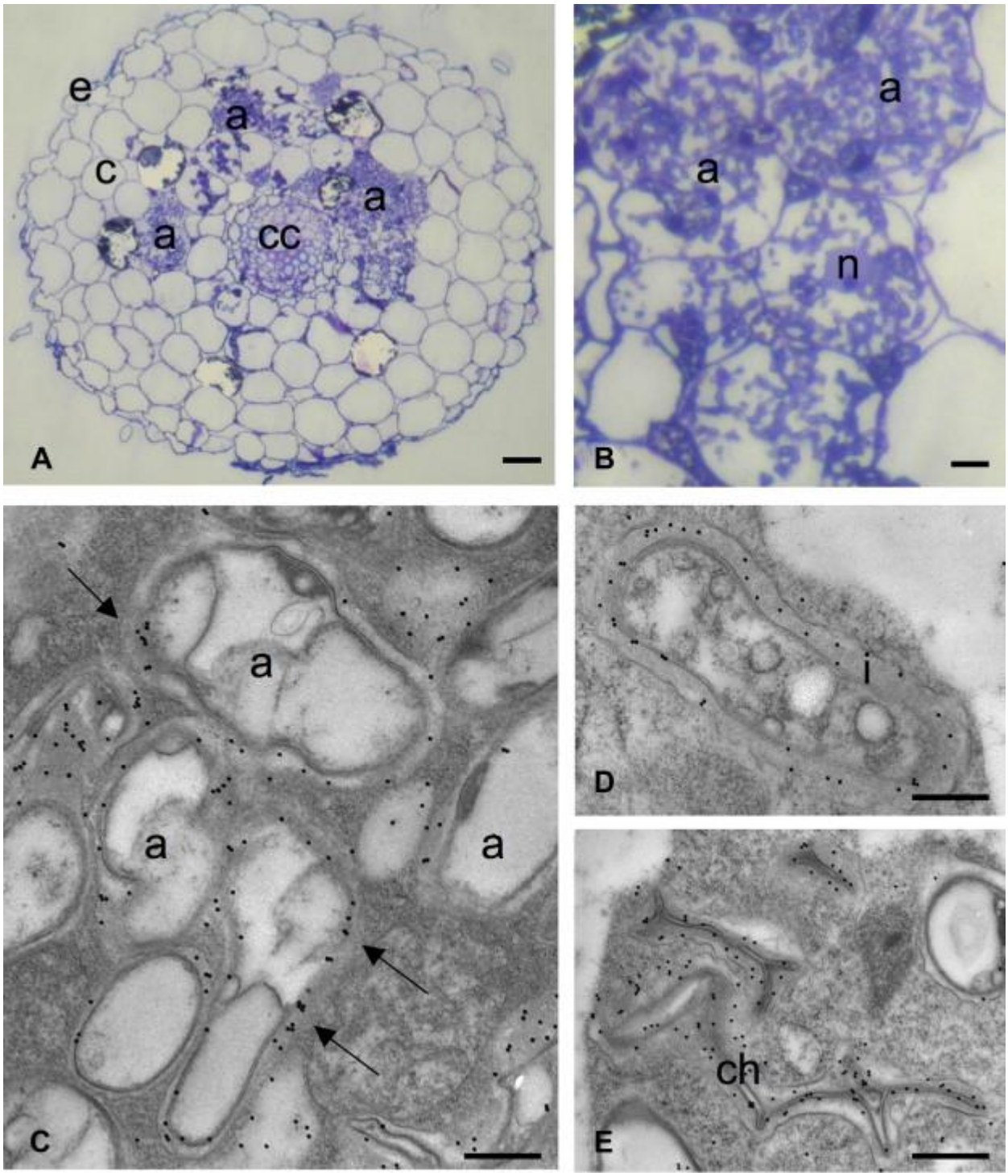

Fig. 5.

Detection of ascorbate oxidase in *L. japonicus* mycorrhizal roots. A. Semithin cross section of *L. japonicus*/*Gi. margarita* mycorrhizal root. Bar = 30 μm a, arbuscule; c, cortical cells; cc, central cylinder; e, epidermal cells. B. Magnification of arbuscules (a). ih, intercellular hyphae. Bar = 6 μm. C–E. Immunogold localization of ascorbate oxidase. C. After treatment with the anti-AO, gold granules are present on the interface space around the fungal branches (arrows). Bar = 0.4 μm. D–E. Labeling is present around the living fungal branches (D) and the collapsed ones (E). Bars = 0.4 μm and 0.5 μm in D and E, respectively. a, arbuscular branches; ch, collapsed hyphae; i, interface space; n, host nucleus.

3. Discussion

This work shows for the first time that the same ascorbate oxidase (AO) gene is induced in symbiotic associations of *L. japonicus* with either rhizobia or AM fungi. Localization, in both cases, of the AO protein in the highly specialized structures at the host–symbiont interface, suggests an important role for this enzyme in the general mechanism of symbiosis. The involvement of AO in AM symbiosis is confirmed by the fact that in *M. truncatula* two genes encoding putative AO proteins are shown to be up-regulated when roots were mycorrhized by two different AM fungi [26]. Higher AO activity could also be detected in roots of *Cucumis sativus* mycorrhized with *Glomus mosseae* (R. Balestrini and M.C. De Tullio, unpublished results).

Previous studies showed that AO expression/activity in bean nodules does not respond to oxidative stresses (salt, Cd, hydrogen peroxide), whereas a dramatic induction occurs upon jasmonate treatment [27]. An indirect antioxidant role of AO has been hypothesized on the basis of its capability to directly reduce molecular oxygen to water without releasing toxic intermediates [2] and [11]. According to this hypothesis, AO would be involved in a general strategy for the control of oxygen concentration at sites of production (photosynthetic cells) and in other situations requiring oxygen control.

LjAO1 expression in nodules and namely in nodule endodermis (Fig. 2) is clearly in line with the hypothesis of AO-dependent regulation of oxygen content. AO could play a significant role in the establishment of the oxygen diffusion barrier (ODB), which limits oxygen access to the inner part of the nodule, where nitrogenase activity takes place. High AO activity in nodule endodermis would reduce oxygen to water, preventing its diffusion to the inner part of the nodule.

Immunolocalisation of AO in intercellular spaces in peripheral nodule cells is also consistent with a role in the control of oxygen diffusion, whereas gold granules associated with the symbiosome and membranous structures suggest a regulated distribution of the protein within the cells.

Apoplastic location (also confirmed by our data) is a key feature of AO. This is potentially very important in the context of symbioses, not only because cell surface is obviously the first point of contact between plant and symbiotic microorganisms, but also because symbiosis requires extensive rearrangements of cell wall structure and function [28] and [29].

AO could be part of the general mechanism regulating cell wall architecture. This is supported by several lines of evidence. As mentioned above, AO activity leads to ASC oxidation to DHA, which is considered the first step of ASC catabolism [30]. Localized oxidation of ASC to DHA could be required to cause controlled cell wall loosening, thus explaining the repeatedly observed connection between AO and cell enlargement [8] and [9]. DHA itself could have an additional role as a signaling molecule [31] and [32].

Data showing the symbiosis-induced expression of *LjAO1* open the way to a number of interesting questions. The molecular mechanism of AM symbiosis is much less characterized than nodule formation, and it is not clear whether AO has exactly the same function in the two symbioses. In nodules, AO is very likely to have both an oxygen-controlling function in the ODB and a role in cell wall rearrangement, whereas in arbuscule-containing cells (where high AO expression was observed) AO is possibly involved in the accommodation of fungal structures, with a role in maintaining the structure of the interface compartment as well as in the cell wall loosening and extension observed in arbusculated cells [29]. Further studies are required to elucidate AO function, especially in the AM symbiosis.

High AO expression and activity were also observed in the root apical meristem, namely in quiescent center cells [33], and also in this case the presence of the enzyme could have a decisive role in obtaining a tightly controlled and localized oxygen decrease. The necessity of ensuring hypoxic conditions to keep cells in an undifferentiated state is a recurring theme in current animal stem cells research [34] and [35]. The presence of AO in the root stem cell niche opens an interesting scenario, deserving additional investigation. It is especially noteworthy that AO is potentially able to regulate not only oxygen, but also AsA availability. Studies by the Foyer group [12] highlighted that controlling AsA extracellular levels may have a regulatory role in intercellular communication, which is probably essential in meristem tissues.

In summary, available evidence supports the hypothesis that AO is involved in different and apparently unrelated aspects of plant development, in connection with oxygen, AsA, cell wall rearrangements and signaling. Further studies are needed to assess the consistency of this model, and to solve the mystery of the widespread presence of AO in the plant kingdom.

4. Materials and methods

4.1. Biological materials

Dried *Lotus* seeds were placed in a reaction tube and 2 volumes of 95–97% sulfuric acid were added. After 10 min incubation, seeds were carefully washed six times with sterile water before being sterilized in a 2% sodium hypochloride solution for 10–20 min. Sterilization time was dependent on the age of the seeds. Afterwards, seeds were again washed six times in sterile water and then placed onto sterile wet filter paper in a Petri dish. Seeds were germinated for at least 3 days at 16/8 h day/night cycle and 22 °C before being transferred onto squared Petri dishes containing ¼ B&D medium [36] for sterile cultivation or into pots containing quarz sand. Plants were grown for two weeks before being inoculated with *M. loti*. Rhizobia were grown for 2 days at 28 °C on a rotary shaker in YMB (containing 6.5% K2HPO4) or TY medium prior to application. The rhizobial mutants, *cgs* and *lpsβ2* [18] as well as the corresponding wild-type strain (Ayac 1 BII) were grown for 2 days in liquid AB medium (see above) containing 30 μg/ml Gentamycin for the mutants. For this experiment plants were grown for two weeks prior to infection. 2 ml of the bacterial suspension were spun down at 6000 g using a bench top centrifuge and the pellet was resuspended in sterile water.

For time course experiments nodulated roots were harvested 0, 0.25, 1, 2, 7, 14 and 21 days post inoculation (dpi). For experiments where isolated nodules of different ages were used, emerging nodules were labeled 1, 2, 3 and 4 weeks after inoculation by marking them with different colors on the plastic lid of the squared Petri dish. Nodules were harvested 4 weeks after inoculation according to their label in separate reaction tubes and frozen in liquid nitrogen immediately.

To obtain tissue for analysis of organ specific expression of target genes, plants were grown for 3 weeks under symbiotic conditions using the vertical plate system. Organs were harvested separately from plants grown on 0.1 mM and on 5.0 mM KNO3. Control plants (non-inoculated) were grown only on 0.1 mM KNO3.

For studies on mycorrhyzed plants, *L. japonicus* seeds (Gifu, WT) were scarified and surface-sterilized for 5 min in concentrated sulfuric acid, washed three times with sterile water, and germinated on water agar in petri dishes. Ten-day-old seedlings were inoculated with *Gigaspora margarita* Becker and Hall (strain deposited in the Bank of European Glomales as BEG 34) by the millipore sandwich method [37]. Three seedlings were placed between two membranes (pore diameter 0.45 μm; Sartorius, Goettingen, Germany), either with 10 or 15 fungal spores or without

any spores. Seedlings with the membranes attached were planted in sterile acid-washed quartz sand in Magenta GA-7 vessels (Sigma Aldrich, Milan, Italy) and grown in a climatic chamber at 20 °C, 60% humidity, with 14 h of light per day, in half-strength Long-Ashton nutrient solution [38] with 20 µM $PO4^{3-}$. After 4 weeks, samples from roots were cut after observation under a stereo microscope. Some segments were stained with 0.1% cotton blue in lactic acid and the infection was quantified as described by Trouvelot et al. [39]; other fragments were processed for cellular and molecular analysis. Root segments from six independent experiments and a total of 30 sandwich cultures were analyzed.

4.2. RNA extraction, cDNA synthesis and RealTime RT-PCR

Plant organs were harvested and immediately frozen in liquid nitrogen in a 2 ml reaction tube. Two clean metal balls were added into every tube and frozen again. Plant material was then ground using a Retsch® mixer mill for 2 min. RNA was extracted from 100 to 200 mg ground tissue using an RNeasy extraction kit. 1 µl of the eluted RNA was run on a 1% agarose gel to check for degradation, and quantity was determined spectrophotometrically at 260 nm. 1 µg of total RNA was used for subsequent cDNA synthesis. Total RNA was mixed with 1 µl 10 × DNase reaction buffer and 1 µl DNaseI (1 U/µl) in a total volume of 10 µl and then incubated for 30 min at room temperature. After inactivation of the enzyme with 1 µl of 50 mM EDTA, 1 µl RNA was run on a 1% agarose gel again in order to check for RNA degradation. In addition Real-time RT-PCR was performed on each sample to test for successful DNA removal using an intron- and an ubiquitin10-specific primer pair:

har1intr2f: 5′- CCTGAAATGCCTATTCGTTGAG-3′,

har1intr2r: 5′- CACAGCTTCTTCTGCATGCG-3′,

LjUbi1f: 5′- TTCACCTTGTGCTCCGTCTTC-3′,

LjUbi1r: 5′- AACAACAGCACACACAGCCAATCC-3′.

Each PCR reaction was carried in out in a total volume of 10 µl containing 1 µl DNase treated RNA, 5 µl 5 × SYBR Green Reaction Mix and 4 µl primer mix (0.5 µM of each primer) using a 384-well Real-Time RT-PCR machine.

After confirmation of successful DNA degradation, cDNA synthesis was performed using SuperScriptIII reverse transcriptase, following the protocol of the supplier (Invitrogen). All RT-PCR steps and calculations of relative transcript amounts were described previously [40].

Mycorrhizal and non-mycorrhizal roots were ground as described before. Due to the difficult root material RNA samples were extracted using the "pine-tree-method" [41]. Integrity of RNA samples was checked using an Agilent 2100 BIOANALYZER. RNA purity was determined by the spectrophotometrical ratios A260nm/A280 nm and A260nm/A230 nm. Removal of genomic DNA was done using the TURBO DNA-*free*™ reagent (Ambion) following the manufacture instructions. Absence of genomic DNA was verified as described above. For Real-time RT-PCR, 1 µg of total RNA was retrotranscibed.

Real-time PCR was carried out with an iCycler apparatus (Bio-Rad) and the following primers were utilized for these experiments:

LjAOXf: 5′ – GCCACATGCTAGAGTTTCCCAA – 3′.

LjAOXr: 5′ – TGTGGTTTTTGCGGAGGCT – 3′.

Each PCR reaction was carried out in a total volume of 20 µl containing 1 µl diluted cDNA (1:5), 10 µl 5 × SYBR Green Reaction Mix and 3 µl of each primer (3 µM) using a 96-well plate.

Single amplicons were produced by both primers sets. A melting curve was recorded at the end of every run to assess amplification product specificity [42]. All reactions were performed for three biological and technical replicates.

4.3. DNA extraction

Plant material (200–300 mg) was ground in liquid nitrogen before 300 µl of CTAB buffer (described above) were added. Samples were incubated for 30 min at 60 °C and mixed once during incubation. 300 µl chloroform:isoamylalcohol (24:1) were then added and the sample carefully mixed followed by 10 min centrifugation at 6000 g at room temperature. The upper phase was transferred to a new tube, 10 mg RNase per ml were added and incubated at 37 °C for 30 min. Afterwards, samples were stored on ice for 5 min before 0.6 volumes of isopropanol were added and DNA was precipitated 1 h to overnight at 20 °C. The DNA was pelleted by centrifugation at 10.600 g for 10 min at 4 °C, the supernatant removed, and the pellet washed with 70% EtOH. After 10 min centrifugation at 4 °C supernatant was removed and DNA pellets were air dried at room temperature. DNA was resuspended in 50 µl TE buffer and stored at −20 °C for further analysis.

4.4. Promoter:GUS fusion analysis

After *in silico* identification of the coding sequence of ascorbate oxidase a putative promoter region of 1046 bp was PCR-amplified using the primers:

AOprom1000fwd 5′-AAGCTTCTTGCTAGTTGGCTAATTTGC-3′ and

AO prom-rev 5′-GGATCCGTTGTTGCTTTTACTTGAAGA-3′.

The forward primer contained a HindIII restriction site while a BamHI site was introduced into the reverse primer. After PCR amplification of the promoter from genomic DNA and HindIII and BamHI restriction, the product was cloned into pBI101 containing the gus-reporter gene 3′ of the multiple cloning site. After obtaining a correctly cloned promoter the construct was transformed into *A. rhizogenes*, which was used for hairy root transformation of *Lotus japonicus* (see below).

4.5. GUS-staining

Plant tissue was placed in an appropriate vessel and covered with GUS-buffer (50 mM sodium phosphate-buffer pH 7.2; 10 mM EDTA; 0.1% Triton X-100; 0.1% Tween 20; 1.05 g/50 ml $K_4(Fe^{II}(CN6))$; 0.83 g/50 ml $K_3(Fe^{III}(CN6))$; 0.5 mg/ml x-Glc). Samples were then placed in a vacuum apparatus and a vacuum was applied three times for 10 min each time. Afterwards, samples were incubated at 37 °C for 12–24 h in the dark before being destained stepwise using 30%, 50%, and 70% ethanol for 10 min per step. Tissue was then stored in 70% ethanol at room temperature.

4.6. Hairy root transformation of lotus japonicus

Seeds were sterilized and germinated as described above (section 2.3). 13-15 seedlings were placed in a square Petri dish containing ½ B5 medium (½ B5 macro-and micronutrients; ½ B5 vitamins; 8 g/l Gelrite; pH 5.2) tilted in a slope way when they reached a length of 0.2–0.5 cm. The root was

inserted into the medium in order to anchor the plant. Plants were grown for 3 days at 21 °C before being transformed. *A. rhizogenes* was injected into the stem of the plant using a fine needle. Bacteria were pre-grown on plates as described above (section 2.3) and resuspended in 4 ml YEB medium to obtain a milky suspension. Infected plants were grown for two weeks before plants with visible hairy roots emerging from the injection site were placed in quarz sand and transferred to a phytotron at 21 °C at 16/8 h light dark rhythm for 3–4 weeks. Plants were inoculated with *M. loti* about 4 days after being transferred into quarz sand.

When antibiotic selection was applied to the plants, wild-type roots were removed from plants two weeks after infection with *A. rhizogenes* and plants were grown for a further 14 days on the ½ B5 medium (described above) containing 25 μg/ml G-418 before being transferred to quartz sand. Further growth was as described above.

4.7. Laser microdissection

Mycorrhizal and non mycorrhizal roots (dissected into 5- to 10-mm segments with a razor blade in the freshly prepared fixative) were fixed in freshly prepared Methacarn (absolute methanol/chloroform/glacial acetic acid 6:3:1) at 4 °C overnight for paraffin embedding [43]. Leica RNase-free PEN-foil slides were used for LMD. Sections of 15-μm thickness were cut using a rotary microtome, and the ribbons were placed and stretched out on the slides with double-distilled (dd)H2O on a 40 °C warming plate. The sections were dried in a 40 °C oven, stored at 4 °C, and used within 2 days. A Leica AS Laser Microdissection system (Leica Microsystems, Inc., Bensheim, Germany) was used to isolate cells from the prepared tissue sections. Just before use, the paraffin sections were deparaffinized in xylen treatment, for 10 min, in 100% ethanol for 2 min, and then air dried. The deparaffinized slides were placed face down on the microscope. The tissues were visualized on a computer monitor through a video camera and the selected cells were dissected as described [43]. The dissection conditions were optimized to obtain a clean, narrow excision of the selected cells: 40-XT objective at power 35 to 45 and speed 3 to 4. The cells subsequently fell into the 0.5-ml RNase-free PCR tube caps located beneath the visualized tissue section. On average, approximately 1,000 to 1700 cell sections were collected in a tube. After collection, approximately 25 μl of RNA extraction buffer from the PicoPure kit (Arcturus Engineering, Mountain View, CA, U.S.A.) was added. Samples were incubated at 42 °C for 30 min, centrifuged at 800 μ*g* for 2 min, and stored at −80 °C. Then, for the following steps of RNA extraction, cells were pooled in a single tube with a final volume of 50 μl. RNA extractions were performed as described in Balestrini et al. (2007). RNA quantification was obtained using the NanoDrop 1000 spectrophotometer. A One-Step RT-PCR kit (Qiagen, Valencia, CA, U.S.A.) was used for the RT-PCR experiments conducted on the RNA extracted from the several samples. Reactions were carried out following the protocol described in Balestrini et al. [43] and amplification reactions were run for 40 cycles. Specific primers for *LjAO1* (LjAOXf and LjAOXr) were used in addition to specific primers for *LjEF1* (TC14054) as housekeeping gene: LjEF1αF, TGTGAAGGATCTCAAGCGTG and LjEF1αR, GTATGGCAATCAAGGACTGG. The PCR products were separated by agarose gel electrophoresis in a Trisacetate-EDTA 0.5X buffer, stained with Ethidium Bromide, and visualized using a VersaDoc Imaging System (Bio-Rad Laboratories, CA, U.S.A.).

4.8. Transmission electron microscopy and immunolabeling

For transmission electron microscopy (TEM), differentiated segments from *L. japonicus* nodules, uninfected and mycorrhizal roots were fixed in 2.5% (v/v) glutaraldehyde in 10 mM Na-phosphate buffer (pH 7.2) overnight at 4 °C. After washing in the same buffer, the were postfixed in 1% (w/v) osmium tetroxide in water for 1 h, washed three times with water, and dehydrated in an ethanol series [30, 50, 70, 90, 100% (v/v); 15 min each step] at room temperature. The samples were

infiltrated in 2:1 (v/v) ethanol/LR White (Polysciences, Warrington, PE, USA) for 1 h, 1:2 (v/v) ethanol/LR White resin for 2 h, 100% LR White overnight at 4 °C and embedded in LR White resin, according to Moore et al. [44]. Semi-thin sections (1 μm) were stained with 1% (w/v) toluidine blue for morphological observations. Thin sections were treated according to the followed immunolocalization protocol. Immunogold labeling with the polyclonal antibody anti-AOX (dilution 1:3000–1:5000) were performed on thin sections as described by Balestrini et al. [45] and observed with a Philips CM10 transmission electron microscope. Labeling specificity was determined by replacing the primary antibody with the buffer. The immunogold experiments were replicated about six times for each treatment.

References

1. Szent-Györgyi On the function of hexuronic acid in the respiration of the cabbage leaf J. Biol. Chem., 90 (1931), pp. 385–393
2. M.C. De Tullio, R. Liso, O. Arrigoni Ascorbic acid oxidase: an enzyme in search of a role Biologia Plantarum, 48 (2004), pp. 161–166
3. M. Sanmartin, P.D. Drogoudi, T. Lyons, I. Pateraki, J. Barnes, A.K. Kanellis Over-expression of ascorbate oxidase in the apoplast of transgenic tobacco results in altered ascorbate and glutathione redox states and increased sensitivity to ozone Planta, 216 (2003), pp. 918–928
4. Yamamoto, M.N. Bhuiyan, R. Waditee, Y. Tanaka, M. Esaka, K. Oba, A.T. Jagendorf, T. Takabe Suppressed expression of the apoplastic ascorbate oxidase gene increases salt tolerance in tobacco and *Arabidopsis* plantsJ. Exp. Bot., 56 (2005), pp. 1785–1796
5. Y. Zhang, H. Li, W. Shu, C. Zhang, W. Zhang, Z. Ye Suppressed expression of ascorbate oxidase gene promotes ascorbic acid accumulation in tomato fruit Plant Mol. Biol. Reporter, 29 (2011), pp. 638–645
6. J. Dowdle, T. Ishikawa, S. Gatzek, S. Rolinski, N. Smirnoff Two genes in *Arabidopsis thaliana* encoding GDP-L-galactose phosphorylase are required for ascorbate biosynthesis and seedling viability Plant J., 52 (2007), pp. 673–689
7. D. Mertz Distribution and cellular localization of ascorbic acid oxidase in the maize root tip Amer. J. Bot., 48 (1961), pp. 405–413
8. L.S. Lin, J.E. Varner Expression of ascorbic acid oxidase in zucchini squash (*Cucurbita pepo* L.) Plant Physiol., 96 (1991), pp. 159–165
9. N. Kato, M. Esaka Expansion of transgenic tobacco protoplasts expressing pumpkin ascorbate oxidase is more rapid than that of wild-type protoplasts Planta, 210 (2000), pp. 1018–1022
10. Pignocchi, J.M. Fletcher, J.E. Wilkinson, J.D. Barnes, C.H. Foyer The function of ascorbate oxidase in tobacco Plant Physiol., 132 (2003), pp. 1631–1641
11. M.C. De Tullio, S. Ciraci, R. Liso, O. Arrigoni Ascorbic acid oxidase is dynamically regulated by light and oxygen. A tool for oxygen management in plants? J. Plant Physiol., 164 (2007), pp. 39–46
12. Pignocchi, G. Kiddle, I. Hernández, S.J. Foster, A. Asensi, T. Taybi, J. Barnes, C.H. Foyer Ascorbate oxidase-dependent changes in the redox state of the apoplast modulate gene transcript accumulation leading to modified hormone signaling and orchestration of defense processes in tobacco Plant Physiol., 141 (2006), pp. 423–435
13. D.B. Layzell, S. Gaito, S. Hunt Mode lof gas exchange and diffusion in legume nodules I. Calculation of gas exchange rates and energy cost of N_2 fixation Planta, 173 (1988), pp. 117–127
14. D.B. Layzell, S. Hunt, G.R. Palmer Mechanism of nitrogenase inhibition in soybean nodules. Pulse-modulated spectroscopy indicates that nitrogenase activity is limited by O_2 Plant Physiol., 92 (1990), pp. 1101–1107

15. J.F. Witty, F.R. Minchin Methods for the continuous measurement of O_2 consumption and H_2 production by nodulate legume root system J. Exp. Bot., 49 (1998), pp. 1041–1047
16. M.M. Kuzma, H. Winter, P. Storer, I. Oresnik, C.A. Atkins, D.B. Layzell The site of oxygen limitation in soybean nodules Plant Physiol., 119 (1999), pp. 399–407
17. T. Ott, J.T. van Dongen, C. Günther, L. Krusell, G. Desbrosses, H. Vigeolas, V. Bock, T. Czechowski, P. Geigenberger, M.K. Udvardi Symbiotic leghemoglobins are crucial for nitrogen fixation in legume root nodules but not for general plant growth and development Curr. Biol., 15 (2005), pp. 531–535
18. A.L. D'Antuono, T. Ott, L. Krusell, V. Voroshilova, R.A. Ugalde, M.K. Udvardi, V.C. Lepek Defects in rhizobial cyclic glucan and lipopolysaccharide synthesis alter legume gene expression during nodule development Mol. Plant Microbe Interact., 21 (2008), pp. 50–60
19. G. Colebatch, G. Desbrosses, T. Ott, L. Krusell, O. Montanari, S. Kloska, J. Kopka, M.K. Udvardi Global changes in transcription orchestrate metabolic differentiation during symbiotic nitrogen fixation in *Lotus japonicus* Plant J., 39 (2004), pp. 487–512
20. P. Gamas, F. Niebel, N. Lescure, J. Cullimore Use of a subtractive hybridization approach to identify new *Medicago truncatula* genes induced during root nodule development Mol. Plant Microbe Interact., 9 (1996), pp. 233–242
21. N.N. Sandal, K. Bojsen, K.A. Marcker A small family of nodule specific genes from soybean Nucleic Acids Res., 15 (1987), pp. 1507–1519
22. J. Stougaard, J.E. Jørgensen, T. Christensen, A. Kühle, K.A. Marcker Interdependence and nodule specificity of cis-acting regulatory elements in the soybean leghemoglobin *lbc3* and *N23* gene promoters Mol. Gen. Genet., 220 (1990), pp. 353–360
23. P. Bonfante, A. Genre, A. Faccio, I. Martini, L. Schause, J. Stougaard, J. Webb, M. Parniske The *Lotus japonicus LjSym4* gene is required for the successful symbiotic infection of root epidermal cells Mol. Plant Microbe Interact., 13 (2000), pp. 1109–1120
24. M. Novero, A. Faccio, A. Genre, J. Stougaard, K.J. Webb, L. Mulder, M. Parniske, P. Bonfante Dual requirement of the *LjSym4* gene for mycorrhizal development in epidermal and cortical cells of *Lotus japonicus* roots New Phytol., 154 (2002), pp. 741–749
25. R. Liso, M.C. De Tullio, S. Ciraci, R. Balestrini, N. La Rocca, L. Bruno, A. Chiappetta, M.B. Bitonti, P. Bonfante, O. Arrigoni Localization of ascorbic acid, ascorbic acid oxidase, and glutathione in roots of *Cucurbita maxima* L J. Exp. Bot., 55 (2004), pp. 2589–2597
26. N. Hohnjec, M.F. Vieweg, A. Pühler, A. Becker, H. Küster Overlaps in the transcriptional profiles of *Medicago truncatula* roots inoculated with two different *Glomus* fungi provide insights into the genetic program activated during arbuscular mycorrhiza Plant Physiol., 137 (2005), pp. 1283–1301
27. J. Loscos, M.A. Matamoros, M. Becana Ascorbate and homoglutathione metabolism in common bean nodules under stress conditions and during natural senescence Plant Physiol., 146 (2008), pp. 182–192
28. N.J. Brewin Plant cell wall remodelling in the rhizobium–legume symbiosis Crit. Rev. Plant Sci., 23 (2004), pp. 293–316
29. R. Balestrini, P. Bonfante The interface compartment in arbuscular mycorrhizae: a special type of plant cell wall? Plant Biosyst., 139 (2005), pp. 8–15
30. M.A. Green, S.C. Fry Vitamin C degradation in plant cells via enzymatic hydrolysis of 4-O-oxalyl-L-threonate Nature, 433 (2005), pp. 83–87
31. C.H. Foyer, G. Noctor Redox homeostasis and antioxidant signaling: a metabolic interface between stress perception and physiological responses Plant Cell, 17 (2005), pp. 1866–1875
32. V. Fotopoulos, M.C. De Tullio, J.D. Barnes, A.K. Kanellis Altered stomatal dynamics in ascorbate oxidase-overexpressing tobacco plants suggest a role for dehydroascorbate signalling J. Exp. Bot., 59 (2008), pp. 729–737

33. M.C. De Tullio, K. Jiang, L.J. Feldman Redox regulation of root apical meristem organization: connecting root development to its environment Plant Physiol. Biochem., 48 (2010), pp. 328–336
34. Mohyeldin, T. Garzón-Muvdi, A. Quiñones-Hinojosa Oxygen in stem cell biology: a critical component of the stem cell niche Cell Stem Cell, 7 (2010), pp. 150–161
35. H.L. Vieira, P.M. Alves, A. Vercelli Modulation of neuronal stem cell differentiation by hypoxia and reactive oxygen species Progr. Neurobiol., 93 (2011), pp. 444–455
36. W.J. Broughton, M.J. Dilworth Control of leghaemoglobin synthesis in snake beans Biochem. J., 125 (1971), pp. 1075–1080
37. M. Giovannetti, C. Sbrana, L. Avio, A.S. Citernesi, C. Logi Differential hyphal morphogenesis in arbuscular mycorrhizal fungi during pre-infection stages New Phytol., 125 (1993), pp. 587–593
38. E.J. Hewitt Sand and Water Culture Methods Used in the Study of Plant Nutrition, Technical Communication No. 22 Commonwealth Bureau, London (1966)
39. Trouvelot, J.L. Kough, V. Gianinazzi-Pearson Mesure du taux de mycorhization VA d'un système radiculaire. Recherche de méthodes d'estimation ayant une signification fonctionnelle V. Gianinazzi-Pearson, S. Gianinazzi (Eds.), Physiological and Genetical Aspects of Mycorrhizae, INRA Press, Paris (1986), pp. 217–221
40. T. Czechowski, R.P. Bari, M. Stitt, W.-R. Scheible, M.K. Udvardi Real-time RT-PCR profiling of over 1400 *Arabidopsis* transcription factors: unprecedented sensitivity reveals novel root- and shoot-specific genes Plant J., 38 (2004), pp. 366–379
41. S. Chang, J. Puryear, J. Cairney A simple and efficient method for isolating RNA from pine trees Plant Mol. Biol. Reporter, 11 (1993), pp. 113–116
42. K.M. Ririe, R.P. Rasmussen, C.T. Wittwer Product differentiation by analysis of DNA melting curves during the polymerase chain reaction Anal. Biochem., 245 (1997), pp. 154–160
43. R. Balestrini, J. Gómez-Ariza, L. Lanfranco, P. Bonfante Laser microdissection reveals that transcripts for five plant and one fungal phosphate transporter genes are contemporaneously present in arbusculated cells Mol. Plant Microbe Interact., 20 (2007), pp. 1055–1062
44. P.J. Moore, K.M.M. Swords, M.A. Lynch, L.A. Staehelin Spatial organization of the assembly pathways of glycoproteins and complex polysaccharides in the golgi apparatus of plants J. Cell Biol., 112 (1991), pp. 589–602
45. R. Balestrini, M.G. Hahn, A. Faccio, K. Mengden, P. Bonfante Differential localization of carbohydrate epitopes in plant cell walls in the presence and absence of arbuscular mycorrhizal fungi Plant Physiol., 111 (1996), pp. 203–213